

This is a repository copy of *Dispersal limitations and historical factors determine the biogeography of specialized terrestrial protists*.

White Rose Research Online URL for this paper:

<https://eprints.whiterose.ac.uk/148666/>

Version: Accepted Version

---

**Article:**

Singer, David, Mitchell, Edward A D, Payne, Richard John et al. (1 more author) (2019) Dispersal limitations and historical factors determine the biogeography of specialized terrestrial protists. *Molecular Ecology*. ISSN 0962-1083

<https://doi.org/10.1111/mec.15117>

---

**Reuse**

Items deposited in White Rose Research Online are protected by copyright, with all rights reserved unless indicated otherwise. They may be downloaded and/or printed for private study, or other acts as permitted by national copyright laws. The publisher or other rights holders may allow further reproduction and re-use of the full text version. This is indicated by the licence information on the White Rose Research Online record for the item.

**Takedown**

If you consider content in White Rose Research Online to be in breach of UK law, please notify us by emailing [eprints@whiterose.ac.uk](mailto:eprints@whiterose.ac.uk) including the URL of the record and the reason for the withdrawal request.

1 **Dispersal limitations and historical factors determine the biogeography of**  
2 **specialized terrestrial protists**

3 David Singer<sup>1,2</sup>, Edward A.D. Mitchell<sup>1,3</sup>, Richard J. Payne<sup>4</sup>, Quentin Blandenier<sup>1,5</sup>, Clément Duckert<sup>1</sup>, Leonardo  
4 D. Fernández<sup>1,6</sup>, Bertrand Fournier<sup>7</sup> Cristián E. Hernández<sup>8</sup>, Gustaf Granath<sup>9</sup>, Håkan Rydin<sup>9</sup>, Luca  
5 Bragazza<sup>10,11,12</sup>, Natalia G. Koronatova<sup>13</sup>, Irina Goia<sup>14</sup>, Lorna I. Harris<sup>15</sup>, Katarzyna Kajukalo<sup>16</sup>, Anush  
6 Kosakyan<sup>17</sup> Mariusz Lamentowicz<sup>16</sup>, Natalia P. Kosykh<sup>13</sup>, Kai Vellak<sup>18</sup>, Enrique Lara<sup>1,5</sup>

7 **Corresponding author:** David Singer, Department of Zoology, Institute of Biosciences, Rua do Matão, Tv. 14,  
8 n101, São Paulo, SP - 05508-090, Brazil, tel: 0041792182426, email: [david.singer.bio@outlook.com](mailto:david.singer.bio@outlook.com)

9 **Affiliations:**

10 <sup>1</sup>Laboratory of Soil Biodiversity, Institute of Biology, University of Neuchâtel, Rue Emile-Argand 11,  
11 CH-2000 Neuchâtel, Switzerland

12 <sup>2</sup>Department of Zoology, Institute of Biosciences, University of São Paulo, 05508-090, Brazil

13 <sup>3</sup>Jardin Botanique de Neuchâtel, Chemin du Perthuis-du-Sault 58, CH-2000 Neuchâtel, Switzerland

14 <sup>4</sup>Environment, University of York, Heslington, York, YO10 5DD, United Kingdom

15 <sup>5</sup>Real Jardín Botánico, CSIC, Plaza de Murillo 2, 28014 Madrid, Spain

16 <sup>6</sup>Centro de Investigación en Recursos Naturales y Sustentabilidad (CIRENYS), Universidad Bernardo  
17 O'Higgins, Avenida Viel 1497, Santiago, Chile

18 <sup>7</sup>Community and Quantitative Ecology Laboratory, Department of Biology, Concordia University,  
19 7141 Sherbrooke Street West, Montreal, QC H4B 1R6, Canada

20 <sup>8</sup>Centro de Investigación en Recursos Naturales y Sustentabilidad (CIRENYS), Universidad Bernardo  
21 O'Higgins, Avenida Viel 1497, Santiago, Chile

22 <sup>9</sup>Department of Ecology and Genetics, Evolutionary Biology Centre, Uppsala University, Norbyvägen  
23 18D, SE-752 36 Uppsala, Sweden.

24 <sup>10</sup>WSL Swiss Federal Institute for Forest, Snow and Landscape Research, Site Lausanne, Station 2, CH-  
25 1015 Lausanne, Switzerland

26 <sup>11</sup>Laboratory of Ecological Systems (ECOS), Ecole Polytechnique Fédérale de Lausanne (EPFL), School  
27 of Architecture, Civil and Environmental Engineering (ENAC), Station 2, CH-1015 Lausanne,  
28 Switzerland

29 <sup>12</sup>Department of Life Science and Biotechnologies, University of Ferrara, Corso Ercole I d'Este 32, I-  
30 44121 Ferrara, Italy

31 <sup>13</sup>Laboratory of Biogeocenology, Institute of Soil Science and Agrochemistry, Siberian Branch of  
32 Russian Academy of Sciences, Ak. Lavrent'ev ave., 8/2, Novosibirsk, 630090 Russia

33 <sup>14</sup>Babeş-Bolyai University, Faculty of Biology and Geology, Department of Taxonomy and Ecology, 42  
34 Republicii Street, RO-400015, Cluj-Napoca, Romania

35 <sup>15</sup>School of Geography and Earth Sciences, McMaster University, General Sciences Building,  
36 Hamilton, Ontario, L8S 4K1, Canada

37 <sup>16</sup>Laboratory of Wetland Ecology and Monitoring, Faculty of Geographical and Geological Sciences  
38 and Department of Biogeography and Paleoecology, Adam Mickiewicz University, Poznań, Poland

39 <sup>17</sup> Institute of Parasitology, Biology Center, Czech Academy of Sciences, Branisovska 1160/31, 37005  
40 Czeske Budejovice, Czech Republic

41 <sup>18</sup>Institute of Ecology and Earth Sciences, Natural History Museum, University of Tartu, Lai St 40,  
42 Tartu 51005, Estonia

43 **Abstract**

44 Recent studies show that soil eukaryotic diversity is immense and dominated by  
45 microorganisms. However, it is unclear to what extent the processes that shape the  
46 distribution of diversity in plants and animals also apply to microorganisms. Major  
47 diversification events in multicellular organisms have often been attributed to long-term  
48 climatic and geological processes, but the impact of such processes on protist diversity has  
49 received much less attention as their distribution has often been believed to be largely  
50 cosmopolitan. Here, we quantified phylogeographic patterns in *Hyalosphenia papilio*, a large  
51 testate amoeba restricted to Holarctic *Sphagnum*-dominated peatlands, to test if the current  
52 distribution of its genetic diversity can be explained by historical factors or by the current  
53 distribution of suitable habitat. Phylogenetic diversity was higher in Western North America,  
54 corresponding to the inferred geographical origin of the *H. papilio* complex, and was lower in  
55 Eurasia despite extensive suitable habitat. These results suggest that patterns of phylogenetic  
56 diversity and distribution can be explained by the history of Holarctic *Sphagnum* peatland  
57 range expansions and contractions in response to Quaternary glaciations that promoted  
58 cladogenetic range evolution, rather than the contemporary distribution of suitable habitats.  
59 Species distributions were positively correlated with climatic niche breadth, suggesting that  
60 climatic tolerance is key to dispersal ability in *H. papilio*. This implies that, at least for large  
61 and specialized terrestrial microorganisms, propagule dispersal is slow enough that historical  
62 processes may contribute to their diversification and phylogeographic patterns and may partly  
63 explain their very high overall diversity.

64 **Keywords**

65 *Hyalosphenia papilio*, phylogeography, *Sphagnum* peatland, protists, Distribution, Holarctic

## 66 **Introduction**

67 The question of whether the same rules structure the diversity of all eukaryotes, micro and –  
68 macroscopic alike, has been the subject of a heated debate since the early 2000's. The  
69 classical paradigm is that “everything is everywhere, but, the environment selects” (Baas-  
70 Becking, 1934). Defenders of this paradigm have argued that geographic barriers are  
71 ineffective in preventing dispersal of microbes (Fenchel, 2005; Finlay, 1998). Other  
72 researchers, while accepting that some microbes do indeed occur worldwide, have argued that  
73 others are clearly restricted to certain regions: the ‘moderate endemism’ model (Foissner,  
74 1999). This argument is based particularly on a limited number of so-called “biogeographic  
75 flagship species”, with conspicuous morphology.

76 The application of barcoding to protists has brought new nuance to the debate (Pawlowski et  
77 al., 2012). Single-cell DNA barcoding studies (Pawlowski et al., 2012) of individual  
78 “morphospecies” are now revealing the existence of numerous “cryptic” biological species  
79 (Singer et al., 2018). Barcoding studies have now demonstrated geographically limited  
80 distributions in soil (Ryšánek, Hřčková, & Škaloud, 2015) freshwater (Škaloud et al., 2019)  
81 and marine organisms (Santoferrara, Rubin, & Mcmanus, 2018), although cases of  
82 cosmopolitan distribution have also been reported (Geisen, Fiore-Donno, Walochnik, &  
83 Bonkowski, 2014; Šlapeta, López-García, & Moreira, 2005). The development of microbial  
84 phylogeography, combining biogeography and molecular phylogeny, in turn allows the  
85 evaluation of possible drivers of diversity patterns, and comparison to those known to drive  
86 plant and animal diversity (Martiny et al., 2006).

87 Among terrestrial microorganisms, testate amoebae are particularly useful models for  
88 phylogeographical studies. Testate amoebae are conspicuous and relatively easy to identify

89 and are also large enough to be isolated individually for DNA barcoding. Many species have  
90 narrow ecological tolerances and thus can only colonize specific, often geographically  
91 discontinuous habitats (Singer et al., 2018). Furthermore, some species have well-documented  
92 distribution and ecology. A good example is *Hyalosphenia papilio*, a widely recorded and  
93 morphologically distinctive testate amoeba taxon (Fig. 1). Of particular interest for  
94 phylogeographic studies is that, based on single cell barcoding and the variable molecular  
95 marker Cytochrome c Oxidase subunit I (COI), *H. papilio* is known to represent a species  
96 complex of at least twelve lineages (Heger, Mitchell, & Leander, 2013).

97 *Hyalosphenia papilio* is found exclusively in Holarctic *Sphagnum*-dominated peatlands  
98 (Amesbury et al., 2018, 2016) and it is known to be absent from similar southern hemisphere  
99 sites despite extensive study (Fernández, Lara, & Mitchell, 2015; Smith, Bobrov, & Lara,  
100 2007). *Sphagnum*-dominated peatlands are comparatively young ecosystems, dating back to  
101 the expansion of boreal and subarctic environments near the Pliocene (Shaw et al., 2010).  
102 *Sphagnum* is an ecosystem engineer that modifies habitats by increasing soil wetness and  
103 decreasing pH and available nutrient content, producing decay-resistant litter rich in phenols  
104 and sphagnum (van Breemen, 1995) and hosting very distinctive prokaryotic, algal and fungal  
105 communities (Kostka et al., 2016; Mutinová, Neustupa, Bevilacqua, & Terlizzi, 2016). Thus,  
106 *Sphagnum* represents a highly selective habitat for macro and microorganisms. This explains  
107 why *Sphagnum*-dominated ecosystems are species-poor and these same factors are likely to  
108 also drive evolutionary adaptations in testate amoebae (Kosakyan et al., 2016; Singer et al.,  
109 2018). Hence, it is likely that this taxon does not pre-date the radiation of peat-forming  
110 *Sphagnum* species between 17 and 7 Mya (Shaw et al., 2010). Large extents of *Sphagnum*  
111 comparable to modern *Sphagnum*-dominated peatlands probably appeared during the late  
112 Miocene/early Pliocene, concomitantly with global cooling, i.e. between 7 and 5.5 Mya

113 (Herbert et al., 2016). While *Sphagnum* occurs at low as well as high latitudes it is only a  
114 dominant component of peatlands in higher latitudes (e.g. Tierra-del-Fuego and the boreal  
115 zone of the Holarctic). The taxonomic richness of the genus is low in the Southern  
116 Hemisphere high latitudes and high in the Northern Hemisphere high latitudes which  
117 correspond to its inferred origin (Shaw, Carter, Aguero, da Costa, & Cowl, 2019).

118 Holarctic *Sphagnum*-dominated peatlands have experienced considerable changes in their  
119 extent due to the repeated advances and retreats of ice sheets during the Quaternary. Many of  
120 the largest areas covered by peatlands today were under ice during the last glacial maximum  
121 (e.g. Fennoscandia, boreal Canada), while peatlands may have persisted in others (e.g. Pacific  
122 coast of Canada)(Treat et al., 2019). These successive glacial expansions and contractions are  
123 known to have shaped genetic diversity in multicellular taxa (Schönswetter, Stehlik,  
124 Holderegger, & Tribsch, 2005), whose dispersal is assumed to be slow in contrast with  
125 eukaryotic microorganisms (Bahram et al., 2016). If, like plants and animals, protist dispersal  
126 is relatively slow, the genetic structure of their populations will bear traces of such range  
127 expansions and contractions. The origin of taxa can potentially be inferred and the timing of  
128 phylogenetic events estimated based on molecular clocks (Arbogast et al., 2006; Arbogast,  
129 Edwards, Wakeley, Beerli, & Slowinski, 2002). On the contrary, fast dispersal in protists  
130 would blur any such signature and taxonomic or phylogenetic diversity would tend to be  
131 distributed randomly and peak in areas with largest extent of favourable habitats (Forest,  
132 Colville, & Cowling, 2018).

133 It follows that the phylogeographical pattern of a given taxon, here *H. papilio*, can be used to  
134 test two alternative hypotheses: 1) Dispersal is low and/or slow enough so that traces of  
135 glacial cycles are reflected in its extant diversity. The highest diversity, and the likely  
136 geographical origin of *H. papilio* would be expected to occur in refugia corresponding to the

137 margins of ice sheets during Last Glacial Maximum where *Sphagnum* peatlands could  
138 survive. 2) Dispersal is high and/or fast, and diversity would be expected to be maximal  
139 where the largest expanses of *Sphagnum* peatlands are found today (e.g. Western Siberia).  
140 Empirical evidence demonstrates a relationship between testate amoeba shell size and  
141 geographic range (Wilkinson, 2001). Population genetics analyses (Lara, Heger, Scheihing, &  
142 Mitchell, 2011) and modelling (Wilkinson, Koumoutsaris, Mitchell, & Bey, 2011) show a  
143 decline in dispersal potential for testate amoebae and theoretical organisms of smaller sizes  
144 (ca. 60  $\mu\text{m}$ ) than that reported for *H. papilio* (size range 90-175 $\mu\text{m}$ ). The ability of entering a  
145 dormant stage (cysts) which can withstand desiccation and other stresses is considered to be a  
146 key dispersal trait in protists (Geisen et al., 2018); however, such structures have never been  
147 reported in *H. papilio*. We therefore predict that the first hypothesis is more likely to be  
148 supported.

149

## 150 **Material and Methods**

### 151 *Dataset preparation*

152 We retrieved all 360 existing COI gene sequences of *H. papilio* from GenBank, together with  
153 information on the origin of the cells from four studies (Gomaa et al., 2014; Heger et al.,  
154 2013; Kosakyan et al., 2012; Oliverio, Lahr, Grant, & Katz, 2015). In addition, we isolated 57  
155 single cells of *H. papilio* from *Sphagnum* samples collected at 13 new sites, targeting under-  
156 sampled regions to compile a global dataset (Supplementary Table 1). Briefly, the cells were  
157 washed three times in autoclaved distilled water before DNA extraction, which was  
158 performed using the guanidine thiocyanate-base protocol (Duckert et al., 2018).  
159 Amplifications of COI gene fragments were performed in two steps: a first PCR was

160 undertaken with the general COI primers LCO1490 and HCO2198 (Folmer, Black, Hoeh,  
161 Lutz, & Vrijenhoek, 1994), which was followed by a nested PCR using, *H. papilio*-specific  
162 primers HPcoiF and HPcoiR (Gomaa et al., 2014). The first DNA amplification profiles  
163 consisted of an initial denaturation step for 3 min at 95°C, followed by 39 cycles of 15 sec of  
164 denaturation at 95°C, 15 sec of annealing at 43°C and 1 min of elongation at 72°C with an  
165 additional final elongation step at 72°C for 10 min. The procedure for the second PCR profile  
166 was the same except that the annealing temperature was increased to 55 °C. Sequencing was  
167 carried out using a BigDye197 Terminator Cycle Sequencing Ready Reaction Kit (Applied  
168 Biosystems) and analysed with an ABI-3130XL DNA sequencer (Applied Biosystems).  
169 Sequences were deposited in GenBank with the following accession numbers: MK823130-  
170 MK823186. COI sequences were edited and aligned (ClustalW algorithm (Thompson,  
171 Gibson, & Higgins, 2002)) using Bioedit (V.7.2.3 (Hall, 1999)). The final dataset including  
172 published and new sequences consisted of 418 sequences from 61 sites (Supplementary Table  
173 1).

#### 174 *Lineage delineation*

175 We delimited genetic lineages following the approach described in Heger (2013). Briefly, to  
176 obtain a general overview of the existing lineages, we first constructed the phylogenetic tree  
177 based on the matrix of the unique sequences (haplotypes) among the 418 considered in this  
178 study. The sequence lengths of the dataset vary from 430 to 620 bp (depending on the primers  
179 used to barcode the isolated cells). We constructed both a Maximum Likelihood (ML) and a  
180 Bayesian tree, with the RAxML algorithm (Stamatakis, Hoover, Rougemont, & Renner,  
181 2008) and MrBayes v. 3.2.6 (Ronquist & Huelsenbeck, 2003), using in both cases a GTR +  $\Gamma$   
182 model. We then tested if the haplotypes were distributed randomly by comparing our  
183 observed distribution with a null model obtained by haplotypes randomly attributed to



184 lineages (10000 replicates). The tree root was placed between two major clades (clade I  
185 contains the lineage L, K, M, J and clade II contains the lineages C, DE, F, B, A, G, H, I) that  
186 appeared well supported in earlier works (Heger et al., 2013; Kosakyan et al., 2012). Bi-  
187 partition support values were evaluated with 1,000 bootstrap replicates. Bayesian MCMC  
188 analysis was carried out with two simultaneous chains and 50,000,000 generations. Trees  
189 were sampled every 1,000 generation and the burn-in was set at 25%. The trees were rooted  
190 internally based on the topology of trees obtained in earlier works (Heger et al., 2013;  
191 Kosakyan et al., 2016), which showed two major clades with maximum support; we rooted  
192 the tree between these two clades. As both trees were congruent, we presented only the ML  
193 tree and used the Bayesian analysis to evaluate the nodes posterior probabilities (pp). We used  
194 three independent methods of lineage delimitation to compare our assignments with those of  
195 Heger 2013: 1) Automatic Barcode Gap Discovery (ABGD) (Fontaneto, Flot, & Tang, 2015;  
196 Puillandre, Lambert, Brouillet, & Achaz, 2011) using the ABGD web-server  
197 <http://www.wabi.snv.jussieu.fr/public/abgd/abgdweb.html>, 2) The sequence divergences using  
198 the Kimura 2-parameter (Kimura, 1980; Nasonova, Smirnov, Fahrni, & Pawlowski, 2010)  
199 using the “ape” package (V3.2 (Paradis, Claude, & Strimmer, 2004)) in R (V3.0.1. (R. Core  
200 Team, 2014)), and 3) GMYC analysis performed with the SPLITS package, version 1.0-19  
201 (Fujisawa & Barraclough, 2013) coded in R, version 3.1.2 (R. Core Team, 2014).

## 202 *Haplotype and lineage network*

203 Haplotypes (defined as genetic units separated by at least a single mutation) were assigned to  
204 the previously determined lineages. Haplotype networks were constructed using minimum  
205 spanning network analysis as implemented in the software PopART (V1.7 (Leigh & Bryant,  
206 2015), Supplementary Table 2). Four main geographical zones (Eastern North America,

207 Western North America, Europe and Asia) were defined to highlight the distribution of the  
208 haplotypes.

### 209 *Historical Biogeography*

210 We first tested whether the observed patterns could be due to chance or to a sampling bias by  
211 calculating the observed beta diversity following (Legendre & De Cáceres, 2013). We then  
212 tested if the observed beta diversity was higher than expected by chance. We simulated beta  
213 diversity values under null expectations and compared them to observed beta diversity values  
214 to obtain p-values and standardized effect sizes. Simulated beta diversity values were  
215 calculated using the same approach (Legendre & De Cáceres, 2013) on a permuted site by  
216 species matrix. Permutations were conducted using the permatswap algorithm of the R-  
217 package “vegan” (Oksanen, Blanchet, & Kindt, 2015) which preserves column sums. This  
218 allows us to randomly attribute species to station while preserving species total abundance.

219 In order to determinate whether species distribution areas were correlated with ecological  
220 tolerance, we determined the climatic niche breadth for each species using the tolerance index  
221 (Dolédec, Chessel, & Gimaret-Carpentier, 2000), with the R package “ade4” (Dray & Dufour,  
222 2007). This index estimates niche breadth based on environmental tolerance (i.e. climate)  
223 (Hurlbert, 1978; Thuiller, 2004) using the dispersion of geographic cells that contain the  
224 target species in the climatic multivariate space. Low values of the index suggest narrow  
225 tolerance while high values correspond to generalists. These indices were inferred based on  
226 geographical coordinates for each occurrence (Supplementary Table 1) and interpolated  
227 climate data sets (Bioclim, 19 variables) that were generated at 2.5 arcmin resolution from  
228 meteorological data (Hijmans, Cameron, Parra, Jones, & Jarvis, 2005). We then estimated  
229 distribution areas of the species based on the number of plots where a given species was

230 observed (i.e. a rough estimate of the spatial range) and plotted it against the estimated  
231 climatic niche breadths.

232 To evaluate the evolutionary events that may explain the current distribution of *H. papilio*  
233 (e.g. dispersal, extinction, range-switching, sympatry, vicariance and founder effect), we  
234 estimated the ancestral distribution and the frequency of event counts in each of 1000  
235 Biogeographic Stochastic Mapping (BSM) analyses, using the BioGeoBEARS package  
236 (Matzke, 2013) in R (V3.0.1. (R. Core Team, 2014)). BioGeoBEARS allows for the  
237 estimation of ancestral geographic ranges on dated phylogeny, comparing several models of  
238 range evolution. We used the DEC model (Ree, Smith, & Baker, 2008) with two free  
239 parameters: "d" (dispersal rate) and "e" (extinction rate), and a fixed cladogenetic model  
240 (cladogenetic event allowed: vicariance, sympatric-subset speciation, and sympatric range-  
241 copying). We also used a DEC model with an extra parameter, "j", which represents the  
242 founder-event speciation, where the new species "jumps" to a range outside of the ancestral  
243 range (DEC + j model). The comparison of these two models was performed using Akaike  
244 Information Criterion (AIC). The age of the nodes of the rescaled BEAST Tree of *H. papilio*  
245 was estimated by constraining its root to 7 Mya, which corresponds to the documented origin  
246 of *Sphagnum* peatlands (Stenøien, Shaw, Shaw, Hassel, & Gunnarsson, 2010), as all known  
247 lineages of *H. papilio* are restricted to these environments. This type of approach has been  
248 used to identify the geographical origin of multicellular taxa of different ages, dispersion  
249 strategies and lifestyles, including hyacinthoid monocots (Ali, Yu, Pfosser, & Wetschnig,  
250 2012), chameleons (Tolley, Townsend, & Vences, 2013) and bees (Trunz, Packer, Vieu,  
251 Arrigo, & Praz, 2016), and is used here, to our knowledge, for the first time in  
252 microorganisms. This approach allowed us to test the two hypotheses: If the frequency of  
253 event counts in each of 1000 BSM sustain low frequency of dispersal events, related to other

254 biogeographic events, the first hypothesis is supported (1.- Dispersal is low and/or slow  
255 enough so that traces of glacial cycles are reflected in its extant diversity), and otherwise, the  
256 second hypothesis is supported (2.- Dispersal is high and/or fast, and diversity would be  
257 expected to be maximal where the largest expanses of *Sphagnum* peatlands are found today).

258

## 259 **Results**

### 260 *Lineage delineation and diversity*

261 The 418 mitochondrial COI sequences of *H. papilio* revealed the existence of 13 or 14 distinct  
262 lineages (Fig. 2). The Kimura 2-parameter test suggested the existence of 14 lineages based  
263 on a threshold of  $\geq 1\%$  sequence divergence. The Generalized Mixed Yule Coalescent  
264 (GMYC) method yielded 13 lineages (lower and upper confidence intervals: 10 and 29  
265 lineages, respectively;  $P = 0.046$ ) based on single threshold methods. Finally, the Automatic  
266 Barcode Gap Discovery (ABGD) method identified 13 lineages, using a distinctive barcoding  
267 gap of 7%. One of these lineages, called here "M" has not been previously recorded. This  
268 lineage was recovered from localities not included in previous studies (i.e. (Gomaa et al.,  
269 2014; Heger et al., 2013; Kosakyan et al., 2012; Oliverio et al., 2015)). It was supported by all  
270 analyses, although the Kimura 2-parameter test suggested dividing it into two (Fig. 2).

271

### 272 *Phylogenetic reconstruction*

273 Sequences from the previously overlooked lineage M diverged from all others ( $pp = 1$ ) and  
274 branched as a sister group to lineages J and K (Fig. 2). Only a single haplotype was retrieved  
275 from Lineage E, and five from lineage D (*sensu* Heger et al. (2013)). Here again the genetic

276 divergence was low (i.e. at most six nucleotides difference between the sequence of lineage E,  
277 and the five sequences of lineage D, all of which were separated by a single nucleotide (Fig.  
278 3)).

279

#### 280 *Haplotype network*

281 The haplotype network (Fig. 3) showed that some lineages (B, H, and L) were composed of  
282 only a single haplotype, whereas others included several haplotypes, independently of the  
283 number of individual cells barcoded. Some lineages were relatively rare (e.g. B, L and M with  
284 seven, two, and seven individuals respectively) whilst others were extensively recorded (e.g.  
285 lineage A was identified more than a hundred times). Null model analyses show that such a  
286 pattern is not expected under random assembly of lineages (Supplementary Fig. 1).

287

#### 288 *Spatial patterns of phylogenetic richness*

289 We found that the observed beta diversity was significantly higher than expected by chance  
290 (SES = 1.71;  $p=0.99$ ), showing a strong spatial structuring of diversity. We also found a  
291 strong positive correlation between niche breadth as estimated using Dolédec tolerance  
292 indices and distribution areas ( $R^2 = 0.75$ ;  $P=0.001$ ). We also found that lineages differed in  
293 their climatic niches with some lineages preferring colder and drier conditions  
294 (Supplementary Fig. 2, lineage H) and others preferring warmer conditions with abundant  
295 precipitation (Supplementary Fig. 2, lineage I).

296 The geographical distribution of phylogenetic richness showed a clear contrast (Fig 1, 3).

297 Only four lineages (A, C, J and G) were recovered from all of Eurasia, five from Eastern

298 North America (A, F, K, J and M), and nine from Western North America (six in Alaska and  
299 five in the Pacific Northwest, only two being shared between these two regions). Thus,  
300 regional as well as overall diversity and diversity turnover were all higher in North America  
301 than in Eurasia.

302 The distribution of the different lineages (Fig. 3) suggests that several haplotypes are specific  
303 to certain geographical areas (B, DE, H, I and L occur only in Western North America, while  
304 K and M occurred only in Eastern North America), whereas others were geographically  
305 widespread (e.g. J is found throughout the Holarctic realm). Null model analyses show that  
306 such a pattern is not expected under random assembly of lineages (Supplementary Fig. 1).  
307 This structure in lineage distribution suggests that geographic dispersal has occurred  
308 comparatively slowly, allowing it to be recovered with a genetic marker such as mtCOI used  
309 for species-level delineation in this group of organisms (Kosakyan et al., 2012).

310

### 311 *Origin of lineages and evaluation of the diversification processes*

312 The AIC selection of biogeographic models implemented in BioGeoBEARS indicated that a  
313 DEC model was the best-supported (Supplementary Table 3). Based on this model, the most  
314 likely ancestral areas for *H. papilio* are in Western North America (Fig. 4). The dispersal  
315 summary extracted from the 1,000 BSM's maps showed that most of the dispersal events  
316 occurred from Western North America and Asia to the other biogeographic areas, and from  
317 Asia to Europe (Supplementary Table 4). The results of the ancestral area estimation and  
318 number of dispersal events analyses showed that the most frequent process during the  
319 historical biogeography of *H. papilio* was narrow sympatry (i.e. when the ancestral range  
320 contains one area, and both daughter lineages inherit that area), followed by a low frequency

321 of dispersal events (range expansion) (Supplementary Fig. 1). The importance of vicariance  
322 and founder events were comparatively limited (Supplementary Fig. 1).

## 323 **Discussion**

### 324 *Diversity and geographical distribution of the lineages and haplotypes*

325 The species complex *H. papilio* is represented by at least 13 lineages in the Holarctic region,  
326 one of which had not been previously described. Although it is possible that some lineages  
327 remain to be discovered, our globally extensive sampling retrieved only one additional  
328 lineage (M), suggesting that we have now captured most of the group's diversity. The genetic  
329 distances determined by our taxon delineating approaches are consistent with the barcoding  
330 gap (<4%) used to discriminate species in other related testate amoebae lineages (e.g. genus  
331 *Nebela*, Hyalospheniidae). The above-mentioned lineages were defined as species under  
332 multiple and independent concepts, including ecological, morphological and evolutionary  
333 (Singer et al., 2018). This might imply that the lineages retrieved in the present study can all  
334 be considered as separate species (Kosakyan, Gomaa, Mitchell, Heger, & Lara, 2013;  
335 Kosakyan et al., 2012; Singer, Kosakyan, Pillonel, Mitchell, & Lara, 2015; Singer et al.,  
336 2018). The accuracy of a species tree built on a single locus may be still questioned,  
337 especially in the case of recent radiations, as the existence of several caveats (like sequencing  
338 pseudogenes, ongoing hybridization processes) cannot be ruled out and may distort the tree's  
339 topology. In Amoebozoa, COI has been chosen as the most accurate marker notably because  
340 of its sensitivity and lack of intra-individual variability (Nassonova et al., 2010) and we  
341 therefore consider it reliable.

342 Lineages of *H. papilio* show different distribution patterns over the Holarctic realm. Four  
343 lineages (J, A, C, G) were found in several regions with contrasted climates (Fig. 1)

344 suggesting that they have a greater ecological tolerance. This is corroborated by the strong  
345 correlation between climatic niche breadth and estimated distribution ranges (Fig. 5),  
346 suggesting that colonization capacity is constrained by specific tolerance to climates. If these  
347 distributional patterns reflect evolutionary adaptation to long-distance dispersal, it would then  
348 imply that the required physiological/lifestyle adaptations to long range migration have  
349 appeared independently at least four times in the history of the *H. papilio* species complex  
350 (Fig. 4).

351 The existence of restricted distributions is even clearer at the haplotype level. Of the 74 total  
352 *H. papilio* haplotypes, only seven (9.2%) were present in two zones, two in three zones  
353 (2.6%) and no single haplotype was found in all four zones. This indicates that even  
354 widespread lineages (e.g. lineage J) show high infra-specific genetic structuring, which  
355 suggests limited gene flow among sites, and thus, geographical isolation (Fernández,  
356 Hernández, Schiaffino, Izaguirre, & Lara, 2017; Lara, Heger, Scheihing, & Mitchell, 2010).

357 Hypothesis 2, that diversity is maximal where the largest expanses of *Sphagnum* peatlands are  
358 found today cannot be supported by our data and analyses. Under this hypothesis, highest  
359 diversity would be expected in regions such as Western Siberia where peatlands are at their  
360 most extensive and cover more than 20% of the landscape (Peregon, Maksyutov, Kosykh, &  
361 Mironycheva-Tokareva, 2008). However, only four “far travelled” lineages were found in the  
362 entire of Eurasia, as compared to 13 in North America. This is despite larger overall area,  
363 more extensive *Sphagnum* peatland extent and an extensive range of climatic conditions. Six  
364 lineages, 50% more than the entire of Eurasia, were found only in Alaska. In contrast, most  
365 genetic diversity seems to be located along the Western North American coast, a region where  
366 peatlands are typically small and scattered today. This fact, together with the strong spatial



367 patterns in lineage distribution observed (Fig. 1, 4) advocates against our hypothesis 2 (fast  
368 dispersal).

### 369 *Geographic origin and influence of historical events*

370 All Eurasian lineages identified were also present in North America, while several lineages  
371 were restricted to North America. This observation alone suggests an American origin for *H.*  
372 *papilio*. Our ancestral range reconstruction corroborates this inference, placing the most  
373 probable origin of the *H. papilio* complex in Western North America (Fig. 4).

374 Dating speciation events is difficult in testate amoebae as their lineages cannot be  
375 morphologically distinguished (Mulot et al., 2017); testate amoeba shell records in peat are  
376 rare before the Holocene. Nevertheless, it is still possible to infer a time window for the  
377 radiation of the lineages indirectly based on the very strict habitat specificity of this taxon. All  
378 lineages of *H. papilio* thus-far identified are restricted to *Sphagnum* peatlands. It is therefore  
379 reasonable to assume that this highly adapted taxon evolved within these ecosystems. The  
380 oldest fossils of genus *Hyalosphenia* were described from the Triassic (*H. baueri* 220 MYA)  
381 (Schönborn, Dörfelt, Foissner, Krienitz, & Schäffer, 1999). *H. baueri* shares some traits like  
382 an “indistinctly vase shape” and the presence of an organic lip surrounding the aperture with  
383 *H. papilio*. However, it is far from clear that both taxa are directly related. Firstly, it has been  
384 shown that the genus *Hyalosphenia* is paraphyletic, as *H. papilio* and *H. elegans* are only  
385 distantly related (Lahr et al., 2019; Lara, Heger, Ekelund, Lamentowicz, & Mitchell, 2008).  
386 Furthermore, a rough calculation can rule out the possibility of a very old age for *H. papilio*.  
387 “Standard” coxI (estimated for animals) mutation rates are typically in the range of a few  
388 percent per million year (Ho & Lo, 2013; Papadopoulou, Anastasiou, & Vogler, 2010),  
389 sometimes much higher (Ney, Frederick, & Schul, 2018). The most divergent *H. papilio*

390 sequences are separated by roughly 10%, which implies that, in order for the deepest  
391 branching in the complex (see Fig. 4) to be 100 MYA old, the mutation rate would need to be  
392 of 0.01% / MYA. This is far below all rates known to date, and even lower than the mutation  
393 rate of cnidarians which are known for their extremely slow evolving mitochondria (Park et  
394 al., 2012). By contrast, to obtain an age of 7 million years the mutation rate would need to be  
395 1.3% / MYA, which is similar to the mutation rate of many arthropods and thus more  
396 parsimonious than the alternative.

397 During the Pleistocene, large areas of North America were intermittently covered by ice  
398 although ice-free refugia remained. The area of *Sphagnum* peatlands likely repeatedly  
399 expanded during inter-glacial periods and contracted in response to glacial periods when ice  
400 masses covered most of the landscape (Shaw et al., 2014). This period is also coetaneous with  
401 most cladogenesis in the *H. papilio* phylogenetic history, which suggests a series of speciation  
402 events by cladogenetic range evolution which may have occurred during interglacial periods  
403 (Fig. 4). Indeed, our analyses show that at least 8 out of 12 cladogenesis events occurred  
404 during the Pleistocene, immediately after the 2.5 MYA boundary (Fig. 4).

405 This hypothesis is also in line with the fact that the BioGeoBears analyses designated narrow  
406 sympatry or the inheritance of the ancestral area of a range by both daughter lineages, as a key  
407 process explaining the distribution of *H. papilio* lineages. At the onset of Quaternary  
408 glaciations (2.58 Mya), one lineage probably existed in Eastern and two in Western North  
409 America (Fig. 4). While the first lineage probably survived south of the ice sheet, where  
410 conditions were wet enough to allow the development of peatlands (Shaw et al., 2010), the  
411 two others were most likely confined to refugia in Western North America.

412 The location of these refugia is known to have shaped the distribution of plants (Eidesen et  
413 al., 2013) and animals (Klüttsch, Manseau, Anderson, Sinkins, & Wilson, 2017). In particular,  
414 Eastern Beringia (today Alaska and Yukon Territory) was wet enough to support the growth  
415 of *Sphagnum* mosses and *Sphagnum* peatlands (Shaw et al., 2013, 2014). These peatlands  
416 allowed the survival of associated organisms, likely including the lineages of *H. papilio*. In  
417 contrast, Western Beringia (today far eastern Russia) was too dry to support large expanses of  
418 *Sphagnum* peatlands (Shaw et al., 2013, 2014) and likely constituted a barrier for the  
419 migration of *H. papilio* westwards. Our data suggest that the colonization of the Palaearctic  
420 region occurred recently, possibly after the last glaciation (Fig. 1). Western Siberia, which  
421 was a cold desert during the Last Glacial Maximum became covered with peatlands after  
422 11000 BP (Velichko, Timireva, Kremenetski, MacDonald, & Smith, 2011) and could have  
423 constituted a bridge that facilitated the invasion of the Western Palaearctic by “far travelled”  
424 lineages of *H. papilio*. Interestingly, a similar pattern has been suggested for the species  
425 *Sphagnum angermanicum* (Stenøien et al., 2010).

426 The present-day distribution of lineages and the local palaeogeographical context designates  
427 Eastern Beringia or the Pacific Coast as the most probable origin for all extant *H. papilio*  
428 lineages. The higher diversity of *H. papilio* haplotypes in North America as compared to  
429 Europe mirrors the higher diversity of vascular plants (Earl Latham & Ricklefs, 1993;  
430 Svenning, 2003), and both were likely similarly driven by glaciations. The phylogeographic  
431 history of *H. papilio*, used here as a convenient model taxon for protists lacking specialised  
432 morphological adaptation for dispersal, thus highlights the importance of historical processes  
433 in explaining the distribution of extant microbial diversity.

434 Thus, following a dispersal event, sympatric diversification could indeed have played a major  
435 role in shaping the current phylogeography of *H. papilio* (Supplementary Fig. 1). It remains to

436 be determined if the case of *H. papilio* is representative for free-living microorganisms in  
437 general. *H. papilio* is large by microbial standards; testate amoebae mostly range between 20  
438 and 200µm and many other protists and most fungi and prokaryotes are smaller. *H. papilio* is  
439 also restricted to *Sphagnum* mosses, which, although widespread across the Holarctic,  
440 nevertheless constitute a very specific habitat. More generalist, smaller species and/or species  
441 possessing structures adapted to dispersal (e.g. fruiting bodies as in many other Amoebozoa,  
442 (Shadwick, Spiegel, Shadwick, Brown, & Silberman, 2009) may show patterns which agree  
443 better with the second hypothesis. Elucidating the historical processes shaping the diversity of  
444 protists with different dispersal strategies, and comparing patterns with better known  
445 macroscopic organisms will open the way to understanding the processes of diversification  
446 that produced the immense diversity existing today.

#### 447 **Acknowledgements**

448 This work was funded by the Swiss NSF (310003A\_143960 & 31003A\_163254) and  
449 intramural project 201730E063 (CSIC) to E.L., the Swiss NSF (P2NEP3\_178543) to D.S., the  
450 Swedish Research Council (VR) (2015-05174) to G.G. and H.R., FONDECYT (11170927)  
451 and UBO/VRIP (170201) to L.D.F., FONDECYT (1170815) to C.E.H and the Russian  
452 Foundation for Basic Research, N 16-55-16007 to N.G.K.. We thank Indrek Hiiesalu for help  
453 during fieldwork, Boris Droz and Christopher Niewoehner (University of North California)  
454 and Matt McGlone (Manaaki Whenua / Landcare Research, Lincoln, NZ) for useful  
455 comments on the manuscript.

456

457

458

459

460 **References**

- 461 Ali, S. S., Yu, Y., Pfosser, M., & Wetschnig, W. (2012). Inferences of biogeographical histories within  
462 subfamily Hyacinthoideae using S-DIVA and Bayesian binary MCMC analysis implemented in  
463 RASP (Reconstruct Ancestral State in Phylogenies). *Annals of Botany*, *109*(1), 95–107. doi:  
464 10.1093/aob/mcr274
- 465 Amesbury, M. J., Booth, R. K., Roland, T. P., Bunbury, J., Clifford, M. J., Charman, D. J., ... Hughes, P. D.  
466 M. (2018). Towards a Holarctic synthesis of peatland testate amoeba ecology: Development  
467 of a new continental-scale palaeohydrological transfer function for North America and  
468 comparison to European data. *Quaternary Science Reviews*, *201*, 483–500.
- 469 Amesbury, M. J., Swindles, G. T., Bobrov, A., Charman, D. J., Holden, J., Lamentowicz, M., ... Payne, R.  
470 J. (2016). Development of a new pan-European testate amoeba transfer function for  
471 reconstructing peatland palaeohydrology. *Quaternary Science Reviews*, *152*, 132–151.
- 472 Arbogast, B. S., Drovetski, S. V., Curry, R. L., Boag, P. T., Seutin, G., Grant, P. R., ... Anderson, D. J.  
473 (2006). The origin and diversification of Galapagos mockingbirds. *Evolution*, *60*(2), 370–382.
- 474 Arbogast, B. S., Edwards, S. V., Wakeley, J., Beerli, P., & Slowinski, J. B. (2002). Estimating divergence  
475 times from molecular data on phylogenetic and population genetic timescales. *Annual*  
476 *Review of Ecology and Systematics*, *33*(1), 707–740.
- 477 Baas-Becking, L. G. M. (1934). *Geobiologie; of inleiding tot de milieukunde*. WP Van Stockum & Zoon  
478 NV.
- 479 Bahram, M., Kohout, P., Anslan, S., Harend, H., Abarenkov, K., & Tedersoo, L. (2016). Stochastic  
480 distribution of small soil eukaryotes resulting from high dispersal and drift in a local  
481 environment. *The ISME Journal*, *10*(4), 885.
- 482 Dolédec, S., Chessel, D., & Gimaret-Carpentier, C. (2000). Niche separation in community analysis: a  
483 new method. *Ecology*, *81*(10), 2914–2927.
- 484 Dray, S., & Dufour, A.-B. (2007). The ade4 package: implementing the duality diagram for ecologists.  
485 *Journal of Statistical Software*, *22*(4), 1–20.
- 486 Duckert, C., Blandenier, Q., Kupferschmid, F. A. L., Kosakyan, A., Mitchell, E. A. D., Lara, E., & Singer,  
487 D. (2018). En garde! Redefinition of *Nebela militaris* (Arcellinida, Hyalospheniidae) and  
488 erection of *Alabasta* gen. nov. *European Journal of Protistology*, *66*, 156–165.
- 489 Earl Latham, R., & Ricklefs, R. E. (1993). Global patterns of tree species richness in moist forests:  
490 energy-diversity theory does not account for variation in species richness. *Oikos*, *67*(2), 325–  
491 333. doi: 10.2307/3545479
- 492 Eidesen, P. B., Ehrich, D., Bakkestuen, V., Alsos, I. G., Gilg, O., Taberlet, P., & Brochmann, C. (2013).  
493 Genetic roadmap of the Arctic: plant dispersal highways, traffic barriers and capitals of  
494 diversity. *New Phytologist*, *200*(3), 898–910. doi: 10.1111/nph.12412
- 495 Fenchel, T. (2005). Cosmopolitan microbes and their ‘cryptic’ species. *Aquatic Microbial Ecology*,  
496 *41*(1), 49–54.
- 497 Fernández, L. D., Hernández, C. E., Schiaffino, M. R., Izaguirre, I., & Lara, E. (2017). Geographical  
498 distance and local environmental conditions drive the genetic population structure of a  
499 freshwater microalga (Bathycocaceae; Chlorophyta) in Patagonian lakes. *FEMS Microbiology*  
500 *Ecology*, *93*(10). doi: 10.1093/femsec/fix125
- 501 Fernández, L. D., Lara, E., & Mitchell, E. A. D. (2015). Checklist, diversity and distribution of testate  
502 amoebae in Chile. *European Journal of Protistology*, *51*(5), 409–424.
- 503 Finlay, B. J. (1998). The global diversity of protozoa and other small species. *International Journal for*  
504 *Parasitology*, *28*(1), 29–48.
- 505 Foissner, W. (1999). Protist diversity: estimates of the near-imponderable. *Protist*, *150*(4), 363–368.
- 506 Folmer, O., Black, M., Hoeh, W., Lutz, R., & Vrijenhoek, R. (1994). DNA primers for amplification of  
507 mitochondrial cytochrome c oxidase subunit 1 from diverse metazoan invertebrates.

508 *Molecular Marine Biology and Biotechnology*, (5). Retrieved from  
509 <http://www.vliz.be/en/imis?refid=64543>

510 Fontaneto, D., Flot, J.-F., & Tang, C. Q. (2015). Guidelines for DNA taxonomy, with a focus on the  
511 meiofauna. *Marine Biodiversity*, 45(3), 433–451. doi: 10.1007/s12526-015-0319-7

512 Forest, F., Colville, J. F., & Cowling, R. M. (2018). Evolutionary diversity patterns in the Cape flora of  
513 South Africa. In *Phylogenetic Diversity* (pp. 167–187). Springer.

514 Fujisawa, T., & Barraclough, T. G. (2013). Delimiting species using single-locus data and the  
515 generalized mixed yule coalescent approach: a revised method and evaluation on simulated  
516 data sets. *Systematic Biology*, 62(5), 707–724. doi: 10.1093/sysbio/syt033

517 Geisen, S., Fiore-Donno, A. M., Walochnik, J., & Bonkowski, M. (2014). *Acanthamoeba* everywhere:  
518 high diversity of *Acanthamoeba* in soils. *Parasitology Research*, 113(9), 3151–3158.

519 Geisen, S., Mitchell, E. A. D., Adl, S., Bonkowski, M., Dunthorn, M., Ekelund, F., ... Lara, E. (2018). Soil  
520 protists: a fertile frontier in soil biology research. *FEMS Microbiology Reviews*, 42(3), 293–  
521 323. doi: 10.1093/femsre/fuy006

522 Gomaa, F., Kosakyan, A., Heger, T. J., Corsaro, D., Mitchell, E. A. D., & Lara, E. (2014). One alga to rule  
523 them all: unrelated mixotrophic testate amoebae (Amoebozoa, Rhizaria and Stramenopiles)  
524 share the same symbiont (Trebouxiophyceae). *Protist*, 165(2), 161–176. doi:  
525 10.1016/j.protis.2014.01.002

526 Hall, T. A. (1999). BioEdit: a user-friendly biological sequence alignment editor and analysis program  
527 for Windows 95/98/NT. *Nucleic Acids Symposium Series*, 41, 95–98.

528 Heger, T. J., Mitchell, E. A. D., & Leander, B. S. (2013). Holarctic phylogeography of the testate  
529 amoeba *Hyalosphenia papilio* (Amoebozoa: Arcellinida) reveals extensive genetic diversity  
530 explained more by environment than dispersal limitation. *Molecular Ecology*, 22(20), 5172–  
531 5184. doi: 10.1111/mec.12449

532 Herbert, T. D., Lawrence, K. T., Tzanova, A., Cleaveland Peterson, L., Caballero-Gill, R., & Kelly, C. S.  
533 (2016). Late Miocene global cooling and the rise of modern ecosystems. *Nature Geoscience*,  
534 9(11), 843–847. doi: 10.1038/ngeo2813

535 Hijmans, R. J., Cameron, S. E., Parra, J. L., Jones, P. G., & Jarvis, A. (2005). Very high resolution  
536 interpolated climate surfaces for global land areas. *International Journal of Climatology*,  
537 25(15), 1965–1978.

538 Ho, S. Y. W., & Lo, N. (2013). The insect molecular clock. *Australian Journal of Entomology*, 52(2),  
539 101–105.

540 Hurlbert, S. H. (1978). The measurement of niche overlap and some relatives. *Ecology*, 59(1), 67–77.

541 Kimura, M. (1980). A simple method for estimating evolutionary rates of base substitutions through  
542 comparative studies of nucleotide sequences. *Journal of Molecular Evolution*, 16(2), 111–  
543 120.

544 Klütsch, C. F. C., Manseau, M., Anderson, M., Sinkins, P., & Wilson, P. J. (2017). Evolutionary  
545 reconstruction supports the presence of a Pleistocene Arctic refugium for a large mammal  
546 species. *Journal of Biogeography*, 44(12), 2729–2739. doi: 10.1111/jbi.13090

547 Kosakyan, A., Gomaa, F., Mitchell, E. A. D., Heger, T. J., & Lara, E. (2013). Using DNA-barcoding for  
548 sorting out protist species complexes: A case study of the *Nebela tinctoria-collaris-bohemica*  
549 group (Amoebozoa; Arcellinida, Hyalospheniidae). *European Journal of Protistology*, 49(2),  
550 222–237. doi: 10.1016/j.ejop.2012.08.006

551 Kosakyan, A., Heger, T. J., Leander, B. S., Todorov, M., Mitchell, E. A. D., & Lara, E. (2012). COI  
552 barcoding of Nebelid testate amoebae (Amoebozoa: Arcellinida): extensive cryptic diversity  
553 and redefinition of the Hyalospheniidae Schultze. *Protist*, 163(3), 415–434. doi:  
554 10.1016/j.protis.2011.10.003

555 Kosakyan, A., Lahr, D. J. G., Mulot, M., Meisterfeld, R., Mitchell, E. A. D., & Lara, E. (2016).  
556 Phylogenetic reconstruction based on COI reshuffles the taxonomy of hyalosphenid shelled

557 (testate) amoebae and reveals the convoluted evolution of shell plate shapes. *Cladistics*,  
558 32(6), 606–623. doi: 10.1111/cla.12167

559 Kostka, J. E., Weston, D. J., Glass, J. B., Lilleskov, E. A., Shaw, A. J., & Turetsky, M. R. (2016). The  
560 *Sphagnum* microbiome: new insights from an ancient plant lineage. *New Phytologist*, 211(1),  
561 57–64.

562 Lahr, D. J. G., Kosakyan, A., Lara, E., Mitchell, E. A. D., Morais, L., Porfirio-Sousa, A. L., ... Kang, S.  
563 (2019). Phylogenomics and morphological reconstruction of Arcellinida testate amoebae  
564 highlight diversity of microbial eukaryotes in the Neoproterozoic. *Current Biology*.

565 Lara, E., Heger, T. J., Ekelund, F., Lamentowicz, M., & Mitchell, E. A. D. (2008). Ribosomal RNA genes  
566 challenge the monophyly of the Hyalospheniidae (Amoebozoa: Arcellinida). *Protist*, 159(2),  
567 165–176.

568 Lara, E., Heger, T. J., Scheihing, R., & Mitchell, E. A. D. (2010). COI gene and ecological data suggest  
569 size-dependent high dispersal and low intra-specific diversity in free-living terrestrial protists  
570 (Euglyphida: *Assulina*). *Journal of Biogeography*, 38(4), 640–650. doi: 10.1111/j.1365-  
571 2699.2010.02426.x

572 Lara, E., Heger, T. J., Scheihing, R., & Mitchell, E. A. D. (2011). COI gene and ecological data suggest  
573 size-dependent high dispersal and low intra-specific diversity in free-living terrestrial protists  
574 (Euglyphida: *Assulina*). *Journal of Biogeography*, 38(4), 640–650.

575 Legendre, P., & De Cáceres, M. (2013). Beta diversity as the variance of community data: dissimilarity  
576 coefficients and partitioning. *Ecology Letters*, 16(8), 951–963.

577 Leigh, J. W., & Bryant, D. (2015). popart: full-feature software for haplotype network construction.  
578 *Methods in Ecology and Evolution*, 6(9), 1110–1116. doi: 10.1111/2041-210X.12410

579 Martiny, J. B. H., Bohannan, B. J. M., Brown, J. H., Colwell, R. K., Fuhrman, J. A., Green, J. L., ... Kuske,  
580 C. R. (2006). Microbial biogeography: putting microorganisms on the map. *Nature Reviews*  
581 *Microbiology*, 4(2), 102.

582 Matzke, N. J. (2013). *Probabilistic historical niogeography: new models for founder-event speciation,*  
583 *imperfect detection, and fossils allow improved accuracy and model-testing* (UC Berkeley).  
584 Retrieved from <https://escholarship.org/uc/item/8227p52c>

585 Mulo, M., Marcisz, K., Grandgirard, L., Lara, E., Kosakyan, A., Robroek, B. J. M., ... Mitchell, E. A. D.  
586 (2017). Genetic determinism vs. phenotypic plasticity in protist morphology. *Journal of*  
587 *Eukaryotic Microbiology*, 64(6), 729–739. doi: 10.1111/jeu.12406

588 Mutinová, P. T., Neustupa, J., Bevilacqua, S., & Terlizzi, A. (2016). Host specificity of epiphytic diatom  
589 (Bacillariophyceae) and desmid (Desmidiaceae) communities. *Aquatic Ecology*, 50(4), 697–709.

590 Nasonova, E., Smirnov, A., Fahrni, J., & Pawlowski, J. (2010). Barcoding amoebae: comparison of  
591 SSU, ITS and COI genes as tools for molecular identification of naked lobose amoebae.  
592 *Protist*, 161(1), 102–115. doi: 10.1016/j.protis.2009.07.003

593 Ney, G., Frederick, K., & Schul, J. (2018). A Post-pleistocene Calibrated Mutation Rate from Insect  
594 Museum Specimens. *PLoS Currents*, 10.

595 Oksanen, J., Blanchet, F. G., & Kindt, R. (2015). *Vegan: commity ecology package. R package version*  
596 2.3-0.

597 Oliverio, A. M., Lahr, D. J. G., Grant, J., & Katz, L. A. (2015). Are microbes fundamentally different than  
598 macroorganisms? Convergence and a possible case for neutral phenotypic evolution in  
599 testate amoeba (Amoebozoa: Arcellinida). *Royal Society Open Science*, 2(12), 150414. doi:  
600 10.1098/rsos.150414

601 Papadopoulou, A., Anastasiou, I., & Vogler, A. P. (2010). Revisiting the insect mitochondrial molecular  
602 clock: the mid-Aegean trench calibration. *Molecular Biology and Evolution*, 27(7), 1659–1672.

603 Paradis, E., Claude, J., & Strimmer, K. (2004). APE: Analyses of Phylogenetics and Evolution in R  
604 language. *Bioinformatics*, 20(2), 289–290. doi: 10.1093/bioinformatics/btg412

605 Park, E., Hwang, D.-S., Lee, J.-S., Song, J.-I., Seo, T.-K., & Won, Y.-J. (2012). Estimation of divergence  
606 times in cnidarian evolution based on mitochondrial protein-coding genes and the fossil  
607 record. *Molecular Phylogenetics and Evolution*, *62*(1), 329–345.

608 Pawlowski, J., Audic, S., Adl, S., Bass, D., Belbahri, L., Berney, C., ... de Vargas, C. (2012). CBOL protist  
609 working group: barcoding eukaryotic richness beyond the animal, plant, and fungal  
610 kingdoms. *PLOS Biology*, *10*(11), e1001419. doi: 10.1371/journal.pbio.1001419

611 Peregon, A., Maksyutov, S., Kosykh, N. P., & Mironycheva-Tokareva, N. P. (2008). Map-based  
612 inventory of wetland biomass and net primary production in western Siberia. *Journal of*  
613 *Geophysical Research: Biogeosciences*, *113*(G1).

614 Puillandre, N., Lambert, A., Brouillet, S., & Achaz, G. (2011). ABGD, Automatic Barcode Gap Discovery  
615 for primary species delimitation. *Molecular Ecology*, *21*(8), 1864–1877. doi: 10.1111/j.1365-  
616 294X.2011.05239.x

617 R. Core Team. (2014). *R: A language and environment for statistical computing*. R Foundation for  
618 *Statistical Computing, Vienna, Austria*. 2013. ISBN 3-900051-07-0.

619 Ree, R. H., Smith, S. A., & Baker, A. (2008). Maximum likelihood inference of geographic range  
620 evolution by dispersal, local extinction, and cladogenesis. *Systematic Biology*, *57*(1), 4–14.  
621 doi: 10.1080/10635150701883881

622 Ronquist, F., & Huelsenbeck, J. P. (2003). MrBayes 3: Bayesian phylogenetic inference under mixed  
623 models. *Bioinformatics*, *19*(12), 1572–1574. doi: 10.1093/bioinformatics/btg180

624 Ryšánek, D., Hřčková, K., & Škaloud, P. (2015). Global ubiquity and local endemism of free-living  
625 terrestrial protists: phylogeographic assessment of the streptophyte alga *Klebsormidium*.  
626 *Environmental Microbiology*, *17*(3), 689–698.

627 Santoferrara, L. F., Rubin, E., & Mcmanus, G. B. (2018). Global and local DNA (meta) barcoding reveal  
628 new biogeography patterns in tintinnid ciliates. *Journal of Plankton Research*, *40*(3), 209–  
629 221.

630 Schönborn, W., Dörfelt, H., Foissner, W., Krienitz, L., & Schäffer, U. (1999). A fossilized microcosmos  
631 in Triassic amber. *Journal of Eukaryotic Microbiology*, *46*(6), 571–584.

632 Schönswetter, P., Stehlik, I., Holderegger, R., & Tribsch, A. (2005). Molecular evidence for glacial  
633 refugia of mountain plants in the European Alps. *Molecular Ecology*, *14*(11), 3547–3555.

634 Shadwick, L. L., Spiegel, F. W., Shadwick, J. D. L., Brown, M. W., & Silberman, J. D. (2009).  
635 *Eumycetozoa= Amoebozoa?*: SSUrDNA phylogeny of protosteloid slime molds and its  
636 significance for the amoebozoan supergroup. *PLoS One*, *4*(8), e6754.

637 Shaw, A. J., Carter, B. E., Aguero, B., da Costa, D. P., & Crowl, A. A. (2019). Range change evolution of  
638 peat mosses (*Sphagnum*) within and between climate zones. *Global Change Biology*, *25*(1),  
639 108–120.

640 Shaw, A. J., Devos, N., Cox, C. J., Boles, S. B., Shaw, B., Buchanan, A. M., ... Seppelt, R. (2010).  
641 Peatmoss (*Sphagnum*) diversification associated with Miocene Northern Hemisphere climatic  
642 cooling? *Molecular Phylogenetics and Evolution*, *55*(3), 1139–1145. doi:  
643 10.1016/j.ympev.2010.01.020

644 Shaw, A. J., Golinski, G. K., Clark, E. G., Shaw, B., Stenøien, H. K., & Flatberg, K. I. (2013).  
645 Intercontinental genetic structure in the amphi-Pacific peatmoss *Sphagnum miyabeanum*  
646 (Bryophyta: Sphagnaceae). *Biological Journal of the Linnean Society*, *111*(1), 17–37. doi:  
647 10.1111/bij.12200

648 Shaw, A. J., Shaw, B., Stenøien, H. K., Golinski, G. K., Hassel, K., & Flatberg, K. I. (2014). Pleistocene  
649 survival, regional genetic structure and interspecific gene flow among three northern peat-  
650 mosses: *Sphagnum inexpectatum*, *S. orientale* and *S. miyabeanum*. *Journal of Biogeography*,  
651 *42*(2), 364–376. doi: 10.1111/jbi.12399

652 Singer, D., Kosakyan, A., Pilonel, A., Mitchell, E. A. D., & Lara, E. (2015). Eight species in the *Nebela*  
653 *collaris* complex: *Nebela gimlii* (Arcellinida, Hyalospheniidae), a new species described from a



654 Swiss raised bog. *European Journal of Protistology*, 51(1), 79–85. doi:  
655 10.1016/j.ejop.2014.11.004

656 Singer, D., Kosakyan, A., Seppey, C. V. W., Pillonel, A., Fernández, L. D., Fontaneto, D., ... Lara, E.  
657 (2018). Environmental filtering and phylogenetic clustering correlate with the distribution  
658 patterns of cryptic protist species. *Ecology*, 99(4), 904–914. doi: 10.1002/ecy.2161

659 Škaloud, P., Škaloudová, M., Doskočilová, P., Kim, J. Im., Shin, W., & Dvořák, P. (2019). Speciation in  
660 protists: Spatial and ecological divergence processes cause rapid species diversification in a  
661 freshwater chrysophyte. *Molecular Ecology*.

662 Šlapeta, J., López-García, P., & Moreira, D. (2005). Global dispersal and ancient cryptic species in the  
663 smallest marine eukaryotes. *Molecular Biology and Evolution*, 23(1), 23–29.

664 Smith, H. G., Bobrov, A., & Lara, E. (2007). Diversity and biogeography of testate amoebae. In *Protist*  
665 *Diversity and Geographical Distribution* (pp. 95–109). Springer.

666 Stamatakis, A., Hoover, P., Rougemont, J., & Renner, S. (2008). A rapid bootstrap algorithm for the  
667 RAxML web servers. *Systematic Biology*, 57(5), 758–771. doi: 10.1080/10635150802429642

668 Stenøien, H. K., Shaw, A. J., Shaw, B., Hassel, K., & Gunnarsson, U. (2010). North American origin and  
669 recent European establishments of the Amphi-Atlantic peat moss *Sphagnum Angermanicum*.  
670 *Evolution*, 65(4), 1181–1194. doi: 10.1111/j.1558-5646.2010.01191.x

671 Svenning, J.-C. (2003). Deterministic Plio-Pleistocene extinctions in the European cool-temperate tree  
672 flora. *Ecology Letters*, 6(7), 646–653. doi: 10.1046/j.1461-0248.2003.00477.x

673 Thompson, J. D., Gibson, T. J., & Higgins, D. G. (2002). Multiple sequence alignment using ClustalW  
674 and ClustalX. *Current Protocols in Bioinformatics*, 2.3.1-2.3.22.

675 Thuiller, W. (2004). Patterns and uncertainties of species' range shifts under climate change. *Global*  
676 *Change Biology*, 10(12), 2020–2027.

677 Tolley, K. A., Townsend, T. M., & Vences, M. (2013). Large-scale phylogeny of chameleons suggests  
678 African origins and Eocene diversification. *Proceedings of the Royal Society of London B:*  
679 *Biological Sciences*, 280(1759), 20130184. doi: 10.1098/rspb.2013.0184

680 Treat, C. C., Kleinen, T., Broothaerts, N., Dalton, A. S., Dommain, R., Douglas, T. A., ... Brovkin, V.  
681 (2019). Widespread global peatland establishment and persistence over the last 130,000 y.  
682 *Proceedings of the National Academy of Sciences*, 116(11), 4822. doi:  
683 10.1073/pnas.1813305116

684 Trunz, V., Packer, L., Vieu, J., Arrigo, N., & Praz, C. J. (2016). Comprehensive phylogeny, biogeography  
685 and new classification of the diverse bee tribe Megachilini: Can we use DNA barcodes in  
686 phylogenies of large genera? *Molecular Phylogenetics and Evolution*, 103, 245–259. doi:  
687 10.1016/j.ympev.2016.07.004

688 van Breemen, N. (1995). How *Sphagnum* bogs down other plants. *Trends in Ecology & Evolution*,  
689 10(7), 270–275. doi: 10.1016/0169-5347(95)90007-1

690 Velichko, A. A., Timireva, S. N., Kremenetski, K. V., MacDonald, G. M., & Smith, L. C. (2011). West  
691 Siberian Plain as a late glacial desert. *Quaternary International*, 237(1–2), 45–53.

692 Wilkinson, D. M. (2001). What is the upper size limit for cosmopolitan distribution in free-living  
693 microorganisms? *Journal of Biogeography*, 28(3), 285–291.

694 Wilkinson, D. M., Koumoutsaris, S., Mitchell, E. A. D., & Bey, I. (2011). Modelling the effect of size on  
695 the aerial dispersal of microorganisms. *Journal of Biogeography*, 39(1), 89–97. doi:  
696 10.1111/j.1365-2699.2011.02569.x

697

698

699

700 **Data Accessibility**

701 The 57 DNA sequences of COI gene of *Hyalophenia papilio* are available in in GenBank with  
702 the following accession numbers: MK823130- MK823186.

703 **Author contributions**

704 D.S., E.A.D.M. and E.L. designed the experiments; D.S., E.A.D.M., G.G., H.R., L.B., N.G.K,  
705 I.G., L.I.H., K.K., M.L., N.P.K., R.J.P. and K.V., collected the samples; D.S., Q.B., C.D.,  
706 L.D.F., B.F., C.E.H. and E.L. analysed the data; D.S., E.A.D.M., R.J.P. and E.L. wrote the  
707 first version of the manuscript, which was then edited by all co-authors.

708 **Conflict of interest**

709 The material in this manuscript is original research, has not been previously published and has  
710 not been submitted for publication elsewhere while under consideration for Molecular  
711 Ecology. We would also like that only the online version appears in colour, as we took special  
712 care in building our figures in a way that they can be read in black and white as well. We have  
713 no conflict of interest in this research.

714

715

716

717

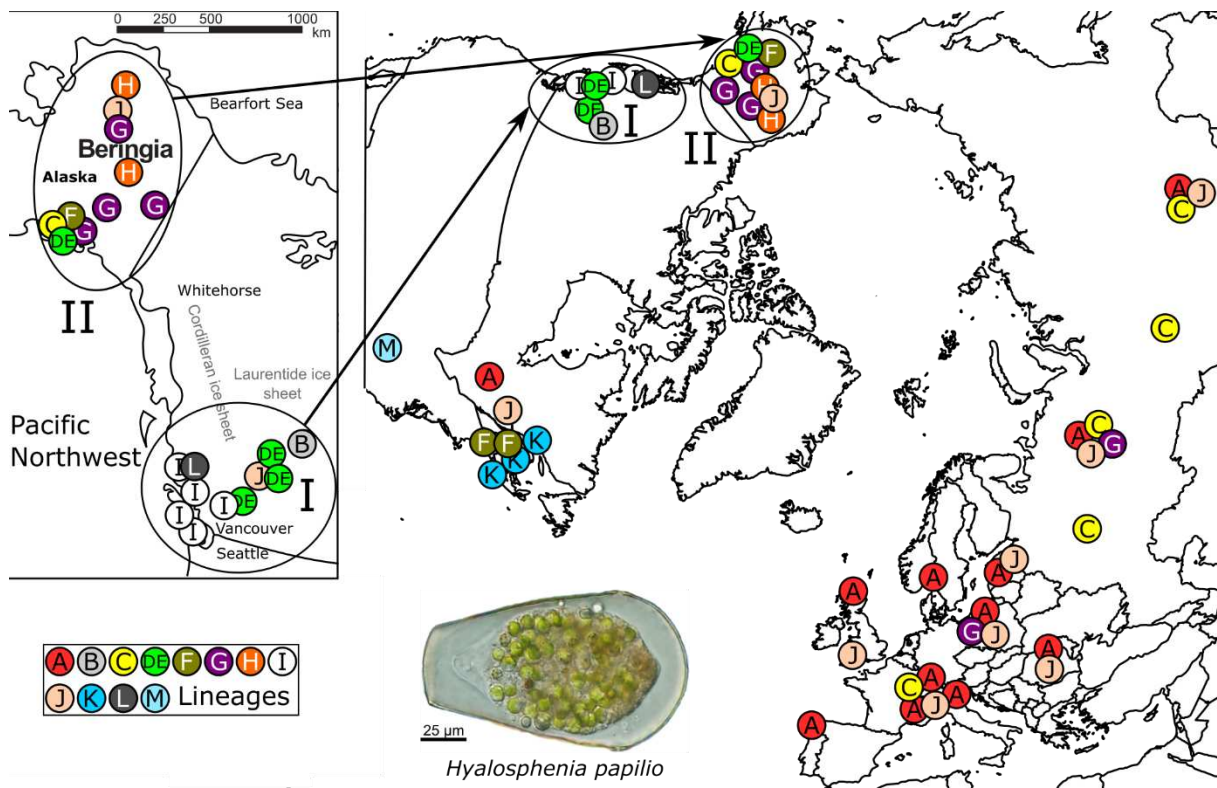
718

719

720

721 **Figures**

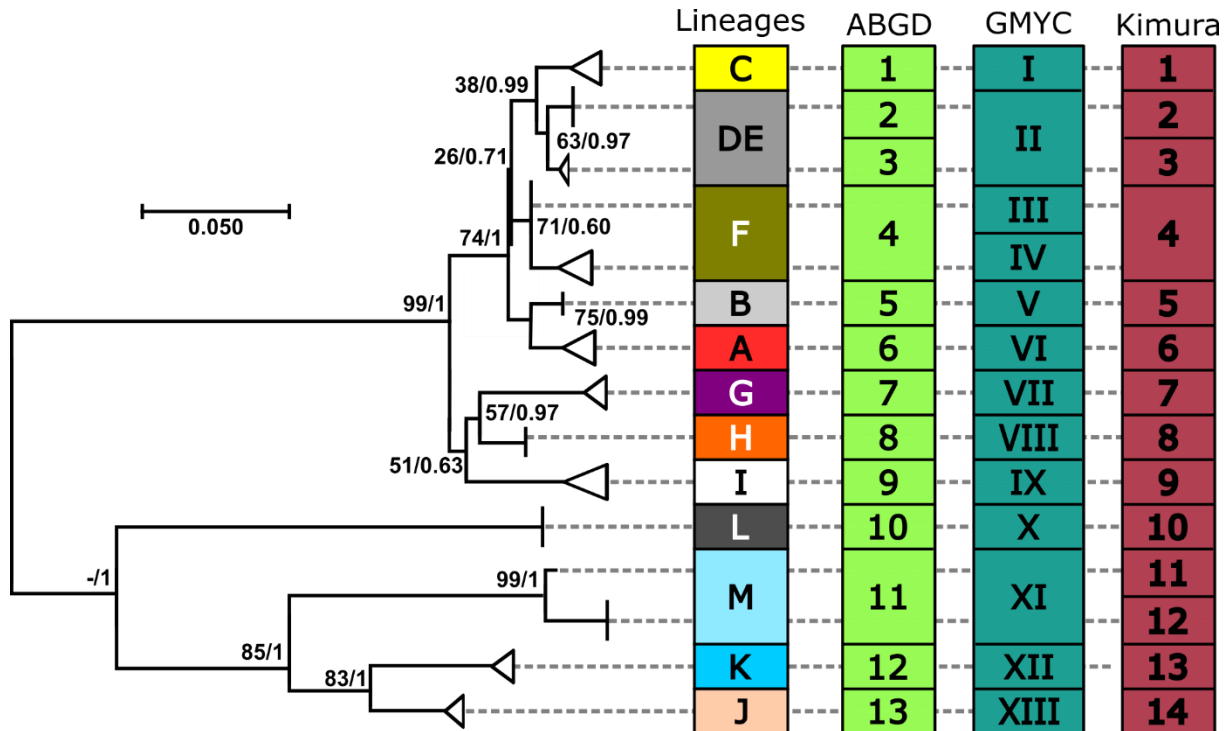
722



723

724 Fig. 1) Holarctic distribution of *Hyalosphenia papilio* lineages. Each circle corresponds to a  
725 sampling site where the lineage has been detected. Lineage codes correspond to phylogenetic  
726 groups, as identified in Heger et al. 2013. I and II present a detailed representation of Beringia  
727 area. Inset: Light microscopy image of *Hyalosphenia papilio*. The pyriform outline  
728 corresponds to the shell that protects the single-cell body of the organism and its  
729 endosymbiotic microalgae (green dots)

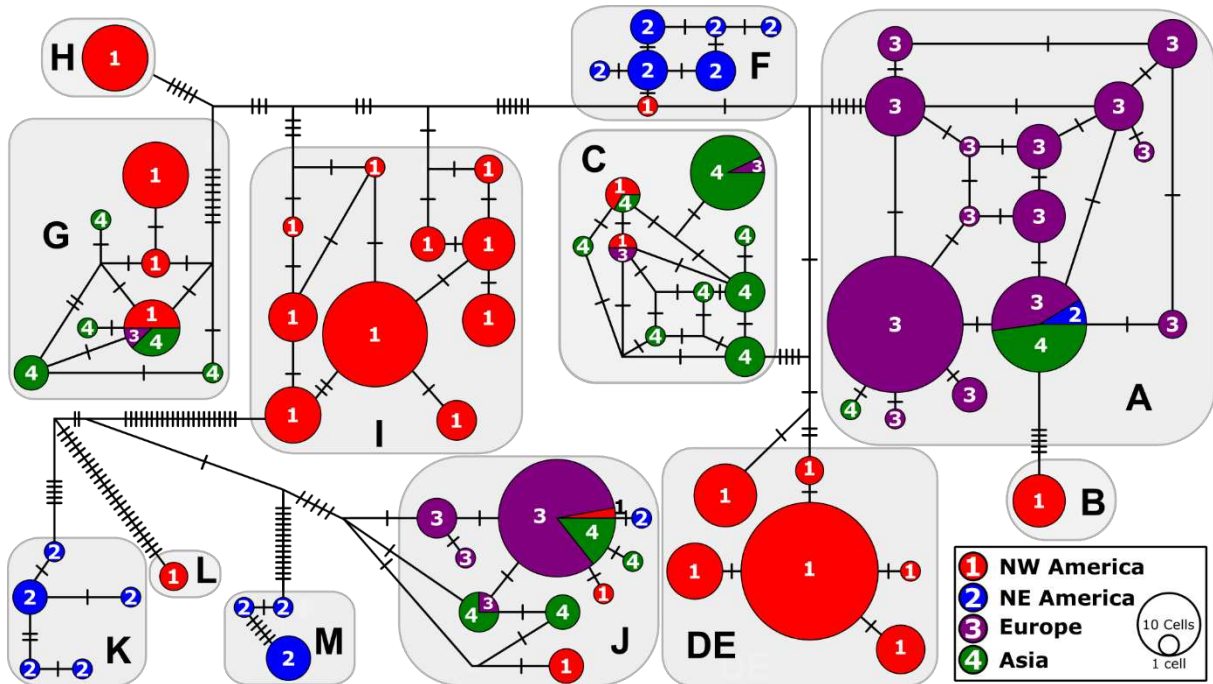
730



731

732 Fig. 2) Maximum Likelihood (ML) and Bayesian concatenated phylogenetic tree from 76  
 733 unique sequences of *Hyalosphenia papilio* isolated from *Sphagnum* peatlands across the  
 734 Holarctic realm. Numbers along branches represent, respectively, bootstraps obtained by ML  
 735 and posterior probabilities as calculated with Bayesian analyses. Trees were rooted internally  
 736 based on the topology of trees obtained in earlier works (Kosakyan et al. 2016, Heger et al.  
 737 2013), which showed two major clades with maximum support; we rooted the tree between  
 738 these two clades. The tree also represents the different lineages obtained with the ABGD and  
 739 GMYC analyses and the Kimura 2-parameter test.

740



741

742 Fig. 3) Median joining haplotype network of cytochrome oxidase subunit 1 (COI) gene of  
 743 *Hyalosphenia papilio* from *Sphagnum* peatlands in the Holarctic realm. Grey boxes and  
 744 letters represent the different lineages identified in the present study. Colours indicate  
 745 geographical regions (legend: bottom right inset). Circle sizes are proportional to the number  
 746 of sequenced single cells of *H. papilio* within each haplotype. Cross lines show the number of  
 747 mutational steps between haplotypes.

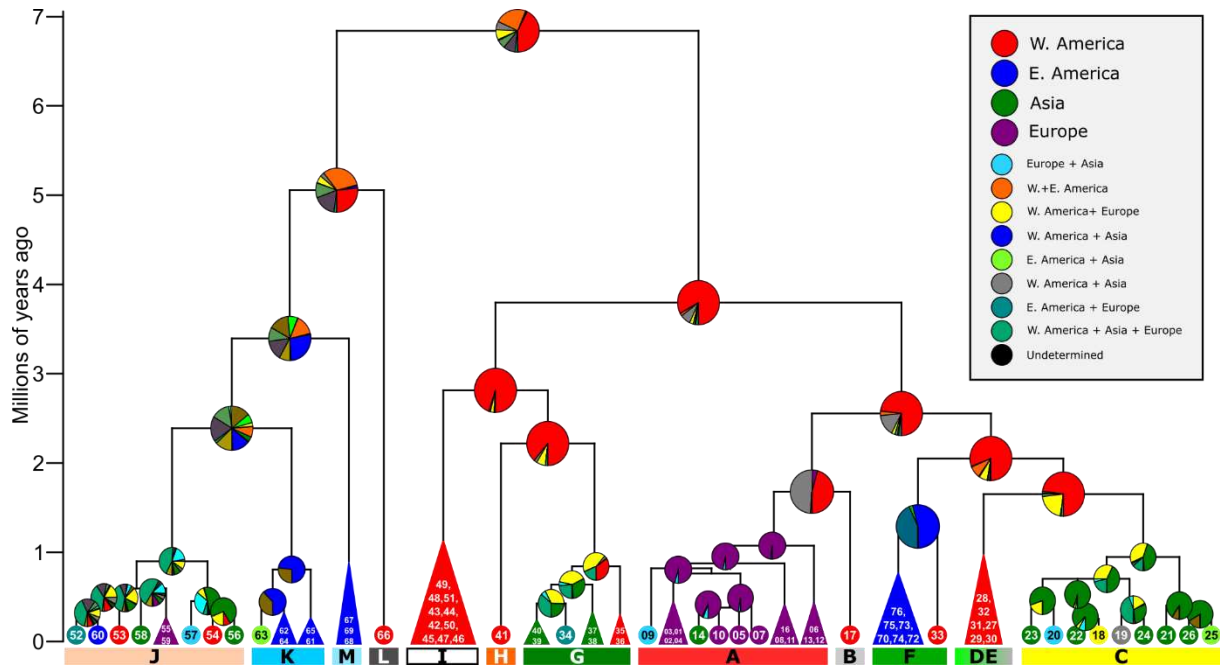
748

749

750

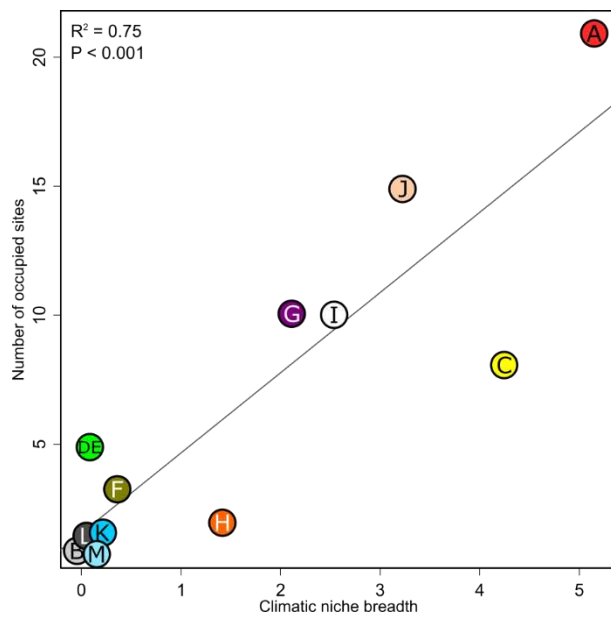
751

752



753

754 Fig. 4) Biogeographical analysis of *H. papilio* from *Sphagnum* peatlands across the Holarctic  
 755 realm using BioGeoBEARS. The four biogeographical areas are: Eastern North America (in  
 756 blue), Western North America (in red), Europe (in purple) and Asia (in green). Pie charts at  
 757 nodes indicate support for each area. The tips are labelled with present-day distributions. The  
 758 secondary colours indicate range combinations of the tip ranges.



759

760 Fig. 5) Relationship of lineage climatic niche breadth to lineage range size (estimated as the  
 761 number of locations where a given lineage is present) of *Hyalosphenia papilio*. Climatic niche  
 762 breadth was estimating from Bioclim variables using the tolerance index of Doledec et al.  
 763 (2000)